# Short Term PV Forecasting Using Satellite Data for Austria

**Dominik Kortschak[1], Marianne Feichtinger-Hofer[1] and Michael Kernitzkyi[1]**

[1] JOANNEUM RESEARCH, Graz (Austria)

**Abstract**

For the grid integration as well as for the integration into smart grids of renewable energies accurate forecasting methods for renewal energies are important. In this paper we consider intraday forecasting of photovoltaic (PV) power production and focus on methods which can be used with satellite data. After a literature review we tested the methods cross correlation (CC), the Bayes method (BM), Variational optical flow (VOF) and persistence (PER) in more detail. With these methods we predict the PV- output for approximately 1500 PV systems in Austria. Finally we present some ideas how the existing methods can be improved and provide first results.

*Keywords: global radiation, forecast, satellite data, photovoltaic*

## 1. Introduction

For the grid integration as well as for the integration into smart grids of renewable energies accurate forecasting methods for renewal energies are of key importance (Kaur et al. 2016; Nonnenmacher et. al 2016). In this paper we concentrate on short term forecasts of photovoltaic (PV) systems. Power forecasts for PV systems can be classified into 3 main methods depending on the data used, i.e. on-site online measurements of PV power, off-site satellite-based or ground-based measurements of global horizontal irradiance (GLO), and NWP-based forecasts. While satellite-based PV prediction uses satellite images to determine the cloud motions field and subsequently possible shadowing of the panel as well as decrease in global horizontal irradiance (GLO) (e.g. Hammer et al., 1999, 2003, Lorenz et al., 2004), ground-based PV prediction uses images from sky imagers (e.g. Chow et al., 2011, 2015, Quesada-Ruiz et al., 2014), fish eye cameras (Chu et al., 2014, 2015b) and sometimes also other data like irradiance measurements from pyranometers and cloud height/distribution from ceilometers as input (Schmidt et al., 2016). The forecast horizon should cover a range of a few minutes to few hours, i.e. nowcasting, to take actions in balancing out the solar power volatility in energy management (Huang et al., 2013). Other forecast methods with larger horizons up to days derive information from NWPs as input and apply post processing methods (e.g. , Larson et al., 2016; Lorenz et al., 2007, 2009, 2011), like sometimes neural networks (e.g. Lauret et al., 2014), since the use of NWPs provide more accuracy in the medium range (Perez et al., 2010).

In this paper we will concentrate on methods that use satellite data. Methods used for satellite-based PV prediction and methods using sky imagers for PV prediction, both depend on motion detection in consecutive images. Hence methods of both branches of the literature are considered in this paper. Popular methods to determine the cloud motion vector field are for example Cross Correlation (e.g. Chow et al., 2011) between two consecutive images, the Bayes method consisting in applying probability functions to different motion fields for determining the most probable vector field (Hammer et al., 2003, Lorenz et al., 2004), Variational Optical Flow by minimization of the energy function of the optical flow field (Chow et al., 2015), sector method by averaging the motion fields over sectors (Quesada-Ruiz et al., 2014) and the use of other motion detection algorithm from the field of computational imaging (Schmidt et al. 2016; West et al. 2014). Most papers use persistence as benchmark and not all used methods are shown to improve over the persistence method.

Whereas determining cloud motion vectors via Cross Correlation (Chow et al., 2011) using sky imager data shows only improvements for very short forecast horizons <5min with respect to persistence, Chow et al. (2015) could derive better forecast results (21-19%) via the Variational Optical Flow method with a fixed smoothness parameter.

Hammer et al. (1999, 2003) and Lorenz et al. (2004) used the HELIOSAT method to derive the ground


doi:10.18086/eurosun2018.09.03 Available at http://proceedings.ises.org

irradiance from satellite-based imagery by correcting the measured irradiance for cloud transmission. Prior to this the satellite images are smoothed and the displacement fields between two consecutive images are determined via probability functions (Bayes method). The one with the maximum probability constitutes the actual cloud motion vector field used for the forecast. Hammer et al. (2003) could show that for point as well as region forecasts this method outperforms persistence and that the optimum size for the smoothing mask applied to the images increases with forecast horizon. Furthermore according to Lorenz et al. (2004), with increasing forecast horizon smoothing becomes even more important for decreasing the forecast error than the methods used, i.e. motion vector estimation (Bayes method) or persistence.

Considering the results for different forecast methods in the literature we choose to concentrate on four existing algorithms namely cross correlation (CC), the Bayes method (BM), Variational optical flow (VOF) and persistence (PER), where from the literature especially (BM) and (VOF) are chosen for their good performance stated in the literature. Besides the algorithms from the literature we also developed a new idea and show first results for this new Algorithm compared to existing ones.

The rest of the paper is organized as follows: In section 2 we describe the used data. In section 3 we describe the used methods from the literature. In section 3 we define a new method for cloud motion forecasts based on affine transformations. In section 5 we provide the used method do calculate power forecasts from global radiation forecasts. In section 6 we provide some information for the implementation of the methods. In section 7 we provide the results of numerical evaluation and finally we add some conclusions in section 8.

## 2. Data

In this paper we use three types of data. We use satellite images, data from NWP and data on feed-in power to the grid.

### *Satellite data*

To test the different state-of-the-art methods for cloud motion estimation we use the global irradiation, cloud height and cloud mask data from the Spinning Enhanced Visible and Infrared Imager (SEVIRI) of the Meteosat Second Generation (MSG, http://msgcpp.knmi.nl/) satellite provided by the Royal Netherlands Meteorological Institute (KNMI). The data covering the period January 2015 to December 2016 has a spatial horizontal resolution of approximately $5 \times 5$ −km and a temporal resolution of 15 minutes. The cloud mask ("cloud area fraction") distinguishes pixels in cloud free, cloud contaminated and cloud filled. The calculation of global horizontal irradiation (GLO; "surface downwelling shortwave flux in air") is based on the Cloud Physical Properties (CPP) algorithm from KNMI.

### *NWP data*

We use the output of the AROME (Application of Research to Operations at MEsoscale) forecast model that is implemented by the ZAMG (Zentralanstalt für Meteorologie und Geodynamik). The model has a special resolution of approximately 2.5 km. For this paper we use global radiation forecasts for the time horizon between January 2015 and December 2016. The forecast are calculated on a daily basis and are available for the next 48 hours with a temporal resolution of 1 hour. This represents a state of the art NWP for Austria.

### *Data on feed-in power*

In this paper we use the feed-in power data of approximately load profile meters of 1497 PV systems all over Austria. The feed-in power data was provided by the APG (Austrian Power Grid) and belongs to the OeMAG Abwicklungsstelle für Ökostrom AG. The feed-in power covers the years 2015 and 2016 and has a temporal resolution of 15 minutes. We have to remark that for each solar power system we have information on the location and on the installed capacity but we don’t have information on the orientation of the solar power panels. Finally we should mention that some of the PV systems only feed-in a part of the produced power. In Fig. 1 we provide a smoothed version of the distribution of the installed kilowatt-peak in Austria we can observe that PV systems usually occur in clusters but are distributed all over Austria.

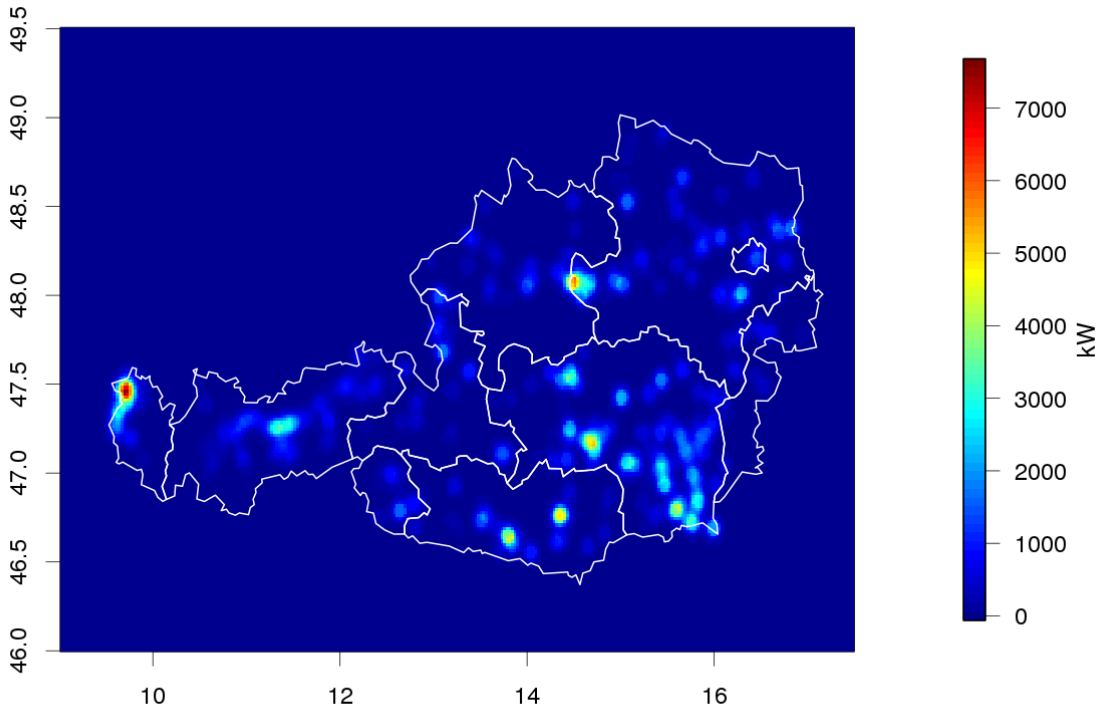


**Fig. 1 Spatial distribution of used PV systems in Austria**

## 3. Description of used state of the art methods for satellite images

We consider cloud motion forecasts from satellite images to generate intraday forecasts of global radiation and feed-in solar power. We decided to implement 4 Methods from the literature: Persistence (PER), Cross Correlation (CC), Variational Optical flow (VOF), and Baysian Method (BM).

Persistence is the simplest method and assumes that cloud cover stays constant at the last observed state. This method is used as benchmark method in most papers.

Cross Correlation: Following (Chow et al. 2011) the cloud motion vector of a sky image can be determined via the cross correlation method (CC) between two consecutive images. We decided to apply the method for blocks with sizes of 41x41 pixels. The reason for this is twofold. First the use of blocks makes the resulting motion field smoother and second reduces the computational load. For every block cross correlation is carried out between a field spanning 41x41 pixels around the block centre of the first image with a shifted pixel field of the same size in the previous image. The maximum displacement is chosen with 9 pixels in each direction corresponding to a maximum wind speed of approximately 180 km/h.

Variational Optical flow: As was stated in Chow et al. (2015) cross correlation does not always improve over the persistence method hence an alternative method was considered in Chow et al. (2015). Chow et al. (2015) use the variational optical flow (VOF) algorithm form (Liu 2009). The principle idea of the algorithm is that the value of a pixel does not change over time but changes location. The VOF method assumes that the pixel intensity remains constant between two consecutive images and only shifts position. The algorithm finds the motion vector that minimizes the difference between the two consecutive satellite images with an additional smoothness constraint on the resulting motion vector. For the estimation we further use a coarse-to-fine warping technique using Gaussian pyramids, meaning that the motion vectors are first calculated at lower resolutions and the motion vector for the lower resolution images is used as starting solution for higher resolution (Liu 2009). In some numerical experiments (not included in this paper) we found that the size of the satellite image can have a significant impact on the performance of the VOF method, meaning that it works better for bigger satellite images.

Bayesian method: The Bayes method described in (Hammer et al. 1999, 2003, 2015; Lorenz et al. 2004; Perez et

al. 2010). The idea of the method is to find the motion vector that maximizes probability given the two consecutive satellite images. Where the probability of a motion vector depends on the difference of the pixel values, the difference in the gradient in the pixels and some smoothness conditions. We applied this method to image fields of 11x11 pixels corresponding to 5 neighbors in each direction

We should highlight the similarity between the BM and VOF method. The principle idea is to find the motion vector of an area that minimizes the difference between the first images and the moved second image. In both methods smoothness of the resulting motion field is also part of the optimization which is the main difference to cross correlation method.

Finally for the implementation we used the programming language R. The methods are implemented according to the cited papers and the references therein.

To make forecasts we first normalize the global radiation from the satellite data with the clear sky index and then apply the motion field repetitively to the normalized global radiation. The clear sky index is finally used to calculate the forecast of the global radiation at a new time point.

## 4. A method using affine transformation

In this section we describe a new method for cloud motion tracking. The principle idea of the method is to track individual cloud systems separately. We will assume that we have two consecutive satellite images image 1 and image 2. The first step is to split the image 1 into areas with similar cloud cover. We will later discuss different possibilities of how the satellite image can be split into different areas. The area basically consists of a set of pixels that can be described by a set of coordinates $I = \{(I_{x,1}, I_{y,1}), \cdots, (I_{x,n}, I_{y,n})\}$. The idea of the method is to find a transformation of the set $I$ to a set $\overline{I}$ such that the difference between the image 1 at set $I$ is close to the values in image 2 of set $\overline{I}$. As possible transformations we will use affine transformations i.e.

$$\overline{I} = A\,I + s \qquad \text{(eq.1)}$$

Where $s = (s_x, s_y)$ is a vector for shifts and $A$ is a $2 \times 2$-Matrix. The calculation of the error and the parameters of the transform are calculated similar as in the VOF algorithm. Meaning at first the image 1 is blurred with a Gaussian filter and evaluated at the index set $I$ the resulting set of values is denoted with $P_I$. The image 2 is evaluated with the help of Gaussian interpolation at the index set $\overline{I}$, we denote the resulting values with $\overline{P_{\overline{I}}}$. As in the VOF algorithm the goal is to minimize

$$\varphi\left(\left(P_I - \overline{P_{\overline{I}}}\right)^2\right) \qquad \text{(eq.2)}$$

where $\varphi(x) = \sqrt{x + 0.001^2}$ is a robust function. As in the VOF algorithm the optimizations is done with the help of a Taylor expansion i.e. For a given start solution of the affine transformation $\overline{I_0}$, we denote with $d\overline{P}^x_{\overline{I_0}}$, $d\overline{P}^y_{\overline{I_0}}$ the derivative of $\overline{P}_{\overline{I_0}}$ in $x$ respectively $y$ direction further for a new solution leading to an image set $\overline{I_n}$ we denote with $dI_n^x, dI_n^y$ the difference between $\overline{I_0}$ and $\overline{I_n}$ in the direction of the $x$ respectively $y$ coordinate. The new affine transformation with leading to the index set $\overline{I_1}$ is than the transformation that minimizes the approximation

$$\varphi\left(\left(P_I - \overline{P_{\overline{I}}} + dI_n^x \cdot d\overline{P}^x_{\overline{I_0}} + dI_n^y \cdot d\overline{P}^y_{\overline{I_0}}\right)^2\right) \qquad \text{(eq.3)}$$

This procedure is iterated until the solution converges or a maximal number of iterations are exceeded.

With the above described method we can calculate for every chosen area a motion vector in direction of the coordinates x and y. The next step is to generate the motion vector for the complete index. In a first step we assigned every pixel the average motion from the different areas in which it is located. For pixels that are in no area a speed of 0 is assumed. Finally a Gaussian filter is used to smooth the wind speeds. If the used areas are not covering the whole satellite image it can be favorable to interpolate the data for pixels outside the chosen areas depending on the distance to other pixel (this can be done with standard methods from spatial kriging). This provides us with motion vectors for the complete satellite image. To get forecasts the methods described in Lorenz (2004) can be used. But we implemented an alternative method where we first calculated for every

chosen area the average motion and translated the complete area by this motion. We then get with the above described method a new motion vector for the complete wind field.

At last we want to describe the method of how to select the areas for the motion vectors. In the first method we normalized the global radiation with the clear sky radiation. This data is then rounded to 4 different values and areas with the same value that are connected together with a buffer are chosen further we discard areas with to view pixels. This method will be referred as AFFINE in the rest of the text. The second method uses the cloud top high for the satellite data determine the areas. As connected areas the connected areas with clouds above 2000m respectively below 2000m are used for the calculations. In this example we get 2 motion fields one for low clouds and one for high clouds. This method will be referred as CloudHigh in the rest of the text.

## 5. From solar forecast to prediction of feed-in power

In section 3 and 4 we have described methods to forecast the global radiation at a given location using satellite images. In this chapter we describe the model that was used to estimate the feed-in power from the global radiation forecasts. We assumed a rather simple model that calculates the infeed data. The main reason for using a simple model is that we are mainly interested in the different performances of the global radiation forecasts and not finding an optimal model for the calculation of feed-in power data from global radiation. Since the main source of error for the feed-in power is usually the error of the global radiation forecast a more sophisticated model would most probably not lead to different results. The model is defined as

$$\frac{P_{out}}{KW_p} = a_1(A,Z)\frac{GLO}{1000} + a_2(A,Z)a_3(CS) + I \quad \text{(eq.4)}$$

where $P_{out}$ is the measured feed-in power in kW, $kW_p$ is the kilowatt peak of the considered PV system, $GLO$ denotes the global radiation, $A$ denotes the azimuth, $Z$ the solar Zenith angle and $CS$ the clear sky radiation. The $a_i$ are continuous functions of the arguments and $I$ is the intercept. We calculated the parameters for each of the 1497 PV systems individually. For the calibration we used the data of the satellite images and we used least squares for the parameters where we additionally added an error term that adds a penalty on the roughness of the functions $a_i$ to avoid overfitting.

## 6. Applications of data

We provide a little more details for the applications of the methods for global radiation forecasts. The implemented methods for global radiation forecasts where applied to satellite images with a spatial extend between 6° and 22° eastern longitude and 43.8° and 51° of northern latitude. We applied the models for the Satellite images with at most 10% of missing data (images are only provided at daylight). With the generated motion vectors we calculate forecasts until the time of the image which has at last less than 50% of missing values. From each forecasts we only used the values for the pixels that correspond to the considered PV systems. We additional added the forecasts of a NWP where we used the average over 30 pixel in each direction instead of the single pixel of the forecast. For the error evaluation we will use the weighted average of the forecasted global radiation. As weights we use the installed kilowatt peak of the PV system.

After calculating the forecasts for the global radiation for the individual PV systems we use the models from section 5 to estimate the feed-in power forecast of the data. The models in section 5 are calibrated with the global radiation data from the satellite images and only the year 2015 is used for the estimation of parameters. For the error calculations we again aggregated the individual PV systems.

With the considered method we have two disadvantages. First satellite images as used in forecasts only exist during daylight. Second we estimated models for individual PV systems, with the aggregation of the model there might be systematic errors in the prediction. To solve the second disadvantage we use generalized additive models with formula SP ~ s(PSP)+s(DT), where $SP$ is the total measured feed-in power, $PSP$ is the predicted feed-in power and $DT$ denotes the time of the day ($s(\cdot)$ means that we consider a smooth function of the variable). To solve the first disadvantage we use the forecast from the NWP meaning that we use the forecast from the NWP whenever no satellite forecast exists. We also used combination of the different models using generalized additive models (COMB). Finally we also tried to incorporate the last known feed-in power. This is again done with generalized additive models and similar to WPPT. This means, that we added a term with the

error of the last known forecast in the generalized additive model. The values are provided for the (COMB) and (NWP) method and are denoted with COMP.C and NWP.C.

## 7. Numerical examples

At first we consider the results for the approximation of the global radiation. In Fig. 2 we provide the normalized mean squared errors (nRMSE). As normalization we use the maximal observed global irradiation. We can observe that the methods using satellite data work better for 2015 than 2016. A possible explanation for this might be different weather conditions in the two years. Interestingly the method using NWP performs better in 2016 than 2015. If we compare the different methods, we can observe that all methods outperform the NWP method for a time horizon of up to 3 hours. Considering the methods based on satellite images, we can observe that the AFFINE method works best followed by the methods CloudHigh, CC, and Bayes, which all work comparable. The methods with the highest nRMSE are the persistence method and the VOF method.

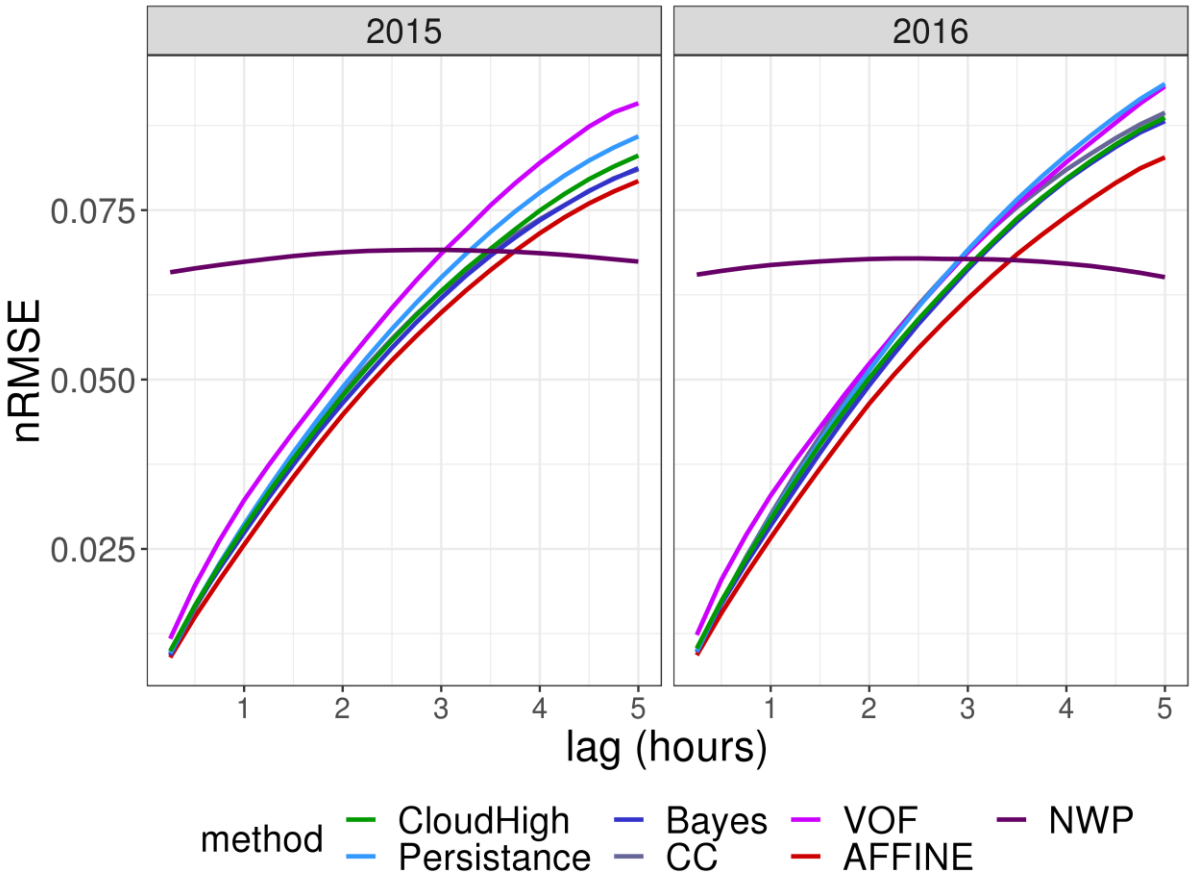


**Fig. 2 Normalized mean squared error (nRMSE) for the prediction of the global radiation**

Next we consider the results for the approximation of the feed-in power in Fig. 3. As normalization we use the installed $kW_p$. We only used time points when forecasts with satellite images where available. In Fig. 3 we added forecasts using the observed satellite data as benchmark (satellite). We can observe that the nRMSE using the satellite decreases for higher lags. The reason for the decreasing of nRMSE is that with increasing lag there are fewer times at which all methods provide forecasts. If we compare the different forecast methods, we can observe that all methods outperform the NWP method for a time horizon of up to 5 hours. Considering the nRMSE of the forecasts methods based on satellite images we can observe a similar order then in Fig. 2 only that especially for 2016 the CloudHigh method outperforms the methods CC, and Bayes. The difference in the ordering of the Fig. 2 and Fig. 3 can be explained by a different weighting of the errors on different times of the

day and that also the satellite measurements are not completely accurate for a considered PV system.

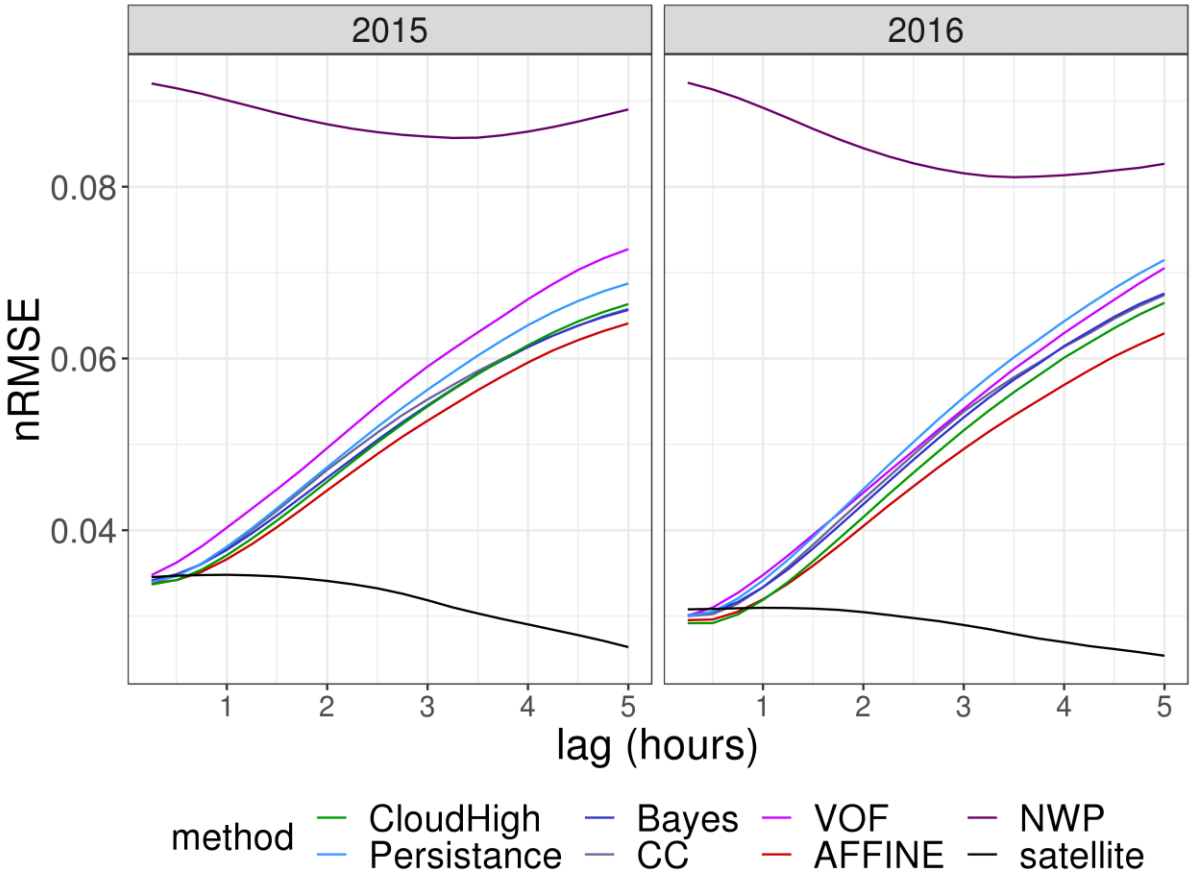


**Fig. 3 Normalized mean squared error (nRMSE) for the prediction of the feed in power**

Finally in Fig. 4 we provide the results for the feed-in power when linear models are applied to the forecasts and for times without data the NWP method is used as well as the combined methods and the methods that are corrected with observed infeed-power. At first we can observe that combining different methods can improve the forecast this especially true for higher lags. Second if we combine forecast with measured feed-in power we can observe that the method can even improve over the measured global radiation from satellite data. The ordering of the other methods is similar as for the results in Fig. 2 and Fig. 3.

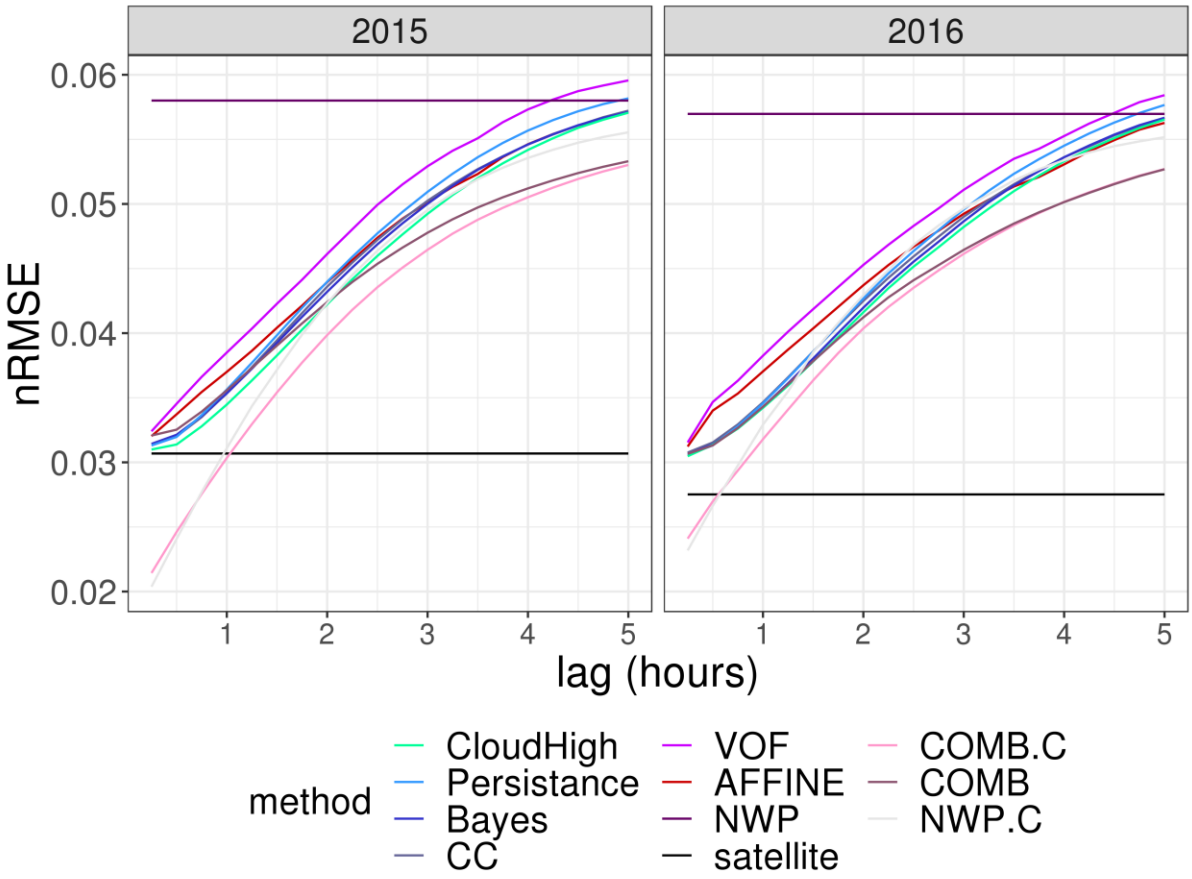


**Fig. 4 Normalized mean squared error (nRMSE) for the prediction of the feed in power**

## 8. Conclusion

In this paper we have considered satellite based PV-forecasts for Austria. We considered the error of the forecasts for the global radiation and for the feed-in power for approximately 1500 PV-systems. We compared the results to a state of the art NWP and tested also the combination of different methods. We have shown that the new method using affine transformation can improve over the other methods that are used in the paper. We can observe that satellite based methods improve over NWP for at least lag of 3 hours. Finally we have seen that combing different methods with linear models and especially adding online measurements can improve the forecasts of individual models (compare Heinemann et al. 2006)

## 9. Acknowledgements

The results are part from the project RESOLW - Renewable Energy Forecast by new Solarradiation- and Windnowcastingsystems which was funded by the Federal Ministry Republic of Austria Transport, Innovation and Technology (BMVIT).

## 10. References

Chow, C.W., Belongie, S., Kleissl, J., 2015. Cloud motion and stability estimation for intra-hour solar forecasting. Solar Energy 115, 645-655. doi: 10.1016/j.solener.2015.03.030

Chow, C.W., Urquhart, B., Lave, M., Dominguez, A., Kleissl, J., Shields, J., Washom, B., 2011. Intra-hour forecasting with a total sky imager at the UC San Diego solar energy testbed. Solar Energy 85(11), 2881-2893. doi: 10.1016/j.solener.2011.08.025

Chu, Y., Pedro, H.T.C., Nonnenmacher, L., Inman, R.H., Liao, Z., Coimbra, C.F.M., 2014. A Smart Image-Based Cloud Detection System for Intrahour Solar Irradiance Forecasts. Journal of Atmospheric and Oceanic Technology 31, 1995-2007. doi: 10.1175/JTECH-D-13-00209.1

Chu, Y., Urquhart, B., Gohari, S.M.I., Pedro, H.T.C., Kleissl, J., Coimbra, C.F.M., 2015. Short-term reforecasting of power output from a 48 MWe solar PV plant. Solar Energy 112, 68-77. doi: 10.1016/j.solener.2014.11.017

Hammer, A., Heinemann, D., Hoyer, C., Kuhlemann, R., Lorenz, E., Müller, R., Beyer, H. G., 2003. Solar energy assessment using remote sensing technologies. Remote Sensing of Environment, 86(3), 423-432. doi: 10.1016/S0034-4257(03)00083-X

Hammer, A., Heinemann, D., Lorenz, E., Lückehe, B., 1999. Short-term forecasting of solar radiation: a statistical approach using satellite data. Solar Energy 67(1), 139-150. doi: 10.1016/S0038-092X(00)00038-4

Hammer, A., Kühnert, J., Weinreich, K., Lorenz, E., 2016. Short-term forecasting of surface solar irradiance based on Meteosat-SEVIRI data using a nighttime cloud index. Remote Sensing 7(7), 9070-9090. doi: 10.3390/rs70709070

Heinemann, D., Lorenz, E., Girodo, M., 2006. Forecasting of solar radiation, in: Dunlop, E.D., Wald, L., Suri, M. (Eds.), Solar energy resource management for electricity generation from local level to global scale. Nova Science Publishers, New York, pp. 83-94.

Huang, H., Xu, J., Peng, Z., Yoo, S., Yu, D., Huang, D., Qin, H., 2013. Cloud motion estimation for short term solar irradiation prediction. IEEE Smart Grid Communications (SmartGridComm) 2013, Symposium, Vancouver, BC, 696-701. doi: 10.1109/SmartGridComm.2013.6688040

Kaur, A., Nonnenmacher, L., Coimbra, C.F., 2016. Net load forecasting for high renewable energy penetration grids. Energy 114, 1073-1084. doi: 10.1016/j.energy.2016.08.067

Liu, C., 2009. Beyond pixels: exploring new representations and applications for motion analysis. doctoral theses, MIT. URL: http://hdl.handle.net/1721.1/53293, last accessed: 13.01.2017

Larson, D.P., Nonnenmacher, L., Coimbra, C.F., 2016. Day-ahead forecasting of solar power output from photovoltaic plants in the American Southwest. Renewable Energy 91, 11-20. doi: 10.1016/j.renene.2016.01.039

Lauret, P., Diagne, M., David, M., 2014. A neural network post-processing approach to improving NWP solar radiation forecasts. Energy Procedia 57, 1044-1052. doi: 10.1016/j.egypro.2014.10.089

Lorenz, E., Hammer, A., Heinemann, D., 2004. Short term forecasting of solar radiation based on satellite data. In proceedings of EuroSun 2004 Congress, Freiburg, Germany, 841-848. URL: https://www.researchgate.net/profile/Annette_Hammer/publication/267971482_Short_term_forecasting_of_solar_radiation_based_on_satellite_data/links/5583ecb708ae4738295bb661.pdf, last accessed: 25.11.2016

Lorenz, E., Heinemann, D., Wichramarathne, H., Beyer, H.G., Bofinger, S., 2007. Forecast of ensemble power production by grid-connected PV systems. In proceedings of 20th European PV Conference, 2007, Milano, Italy URL: https://uol.de/fileadmin/user_upload/physik/ag/ehf/enmet/publications/solar/conference/2007/eupv_milano/forecast_of_ensemble_power_production_by_grid_connected_pv_systems.pdf last accessed: 24.11.2016

Lorenz, E., Scheidsteger, Th., Hurka, J., Heinemann, D., Kurz, C., 2011. Regional PV power prediction for improved grid integration. Prog. Photovolt: Res. Appl. 19, 757-771. doi: 10.1002/pip.1033

Lorenz, E., Remund, J., Müller, S.C., Traunmüller, W., Steinmaurer, G., Pozo, D., Ruiz-Arias, J.A., Faneo, V.L., Ramirez, M.G., Kurz, C., Pomares, L.M., Guerrero, C., 2009. Benchmarking of Different Approaches to Forecast Solar Radiation. 24th European Photovoltaic Solar Energy Conference, 2009, Hamburg, Germany. URL: http://task3.iea-shc.org/data/sites/1/publications/24th_EU_PVSEC_5BV.2.50_lorenz_final.pdf, last accessed: 25.11.2016

Nonnenmacher, L., Kaur, A., Coimbra, C. F., 2016. Day-ahead resource forecasting for concentrated solar power integration. Renewable energy 86, 866-876. doi: 10.1016/j.renene.2015.08.068

Perez, R., Kivalov, S., Schlemmer, J., Hemker, K., Renné, D., Hoff, T.E., 2010. Validation of short and medium term operational solar radiation forecasts in the US. Solar Energy 84, 2161-2172. doi: 10.1016/ j.solener.2010.08.014

Quesada-Ruiz, S., Chu, Y., Tovar-Pescador, J., Pedro, H.T.C., Coimbra, C.F.M., 2014. Cloud-tracking methodology for intra-hour DNI forecasting. Solar Energy 102, 267-275. doi: 10.1016/j.solener.2014.01.030

Schmidt, T., Kalisch, J., Lorenz, E., Heinemann, D., 2016. Evaluating the spatio-temporal performance of sky-imager-based solar irradiance analysis and forecasts. Atmospheric Chemistry and Physics 16(5), 3399-3412. doi: 10.5194/acp-16-3399-2016

West, S.R., Rowe, D., Sayeef, S., Berry, A., 2014. Short-term irradiance forecasting using skycams: motivation and development. Solar Energy 110, 188-207. doi: 10.1016/j.solener.2014.08.038